



# Effect of particle rotation on the drift velocity for nonspherical aerosol particles



George W. Mulholland<sup>a,b,\*</sup>, Charles R. Hagwood<sup>a</sup>, Mingdong Li<sup>b</sup>,  
Michael R. Zachariah<sup>a,b</sup>

<sup>a</sup> National Institute of Standards and Technology, Gaithersburg, MD, USA

<sup>b</sup> University of Maryland, College Park, MD, USA

## ARTICLE INFO

### Article history:

Received 21 August 2015

Received in revised form

7 March 2016

Accepted 17 April 2016

Available online 11 July 2016

### Keywords:

Drift velocity

Rotation velocity

Nonspherical aerosol particles

Nanorod

Translational diffusion coefficient

Free molecular limit

## ABSTRACT

The theoretical drift velocity of a randomly oriented nonspherical aerosol particles in an external field has been previously computed both in the limit of slow rotation and in the limit of fast rotation but not in the intermediate interval. The low rotation limit has been widely used to calculate the drift velocity for a range of nonspherical particles. The fast rotation limit, which is equivalent to the projected area method, has been used for molecular ions and agglomerates. A 1-D model equation containing the particle acceleration and an orientation dependent friction coefficient is proposed to predict the drift velocity between the two limits. This model has the essential physical phenomena without the complications of the 3-D treatment of the combined translation and rotation behavior. As an example, the drift velocity is computed for model parameters based on the friction tensor and rotational diffusion coefficient for circular cross section nanorods in the free molecular limit. For a momentum accommodation coefficient of 0.9 and a particle density of 1000 kg/m<sup>3</sup>, the largest percent deviation from the low rotation velocity limit is 14% and the deviation is at most 1% for nanorods of any length for diameters of 20 nm diameter or larger. Much larger changes in the velocity ratio are shown to occur if the momentum accommodation coefficient is reduced. Also, examples are given where the dimensionless rotation rate increases by about a factor of 7 from either a change in density or a change in the mean free path of the background gas. The results of recent experiments and model calculation of the collision cross section and mobilities of large molecular ions are discussed in regard to our model predictions on the effect of rotation on the drift velocity.

© 2016 Elsevier Ltd. All rights reserved.

## 1. Introduction

A commonly used method for characterizing the size of aerosol particles is based on their mobility derived from the measurement of their drift velocity under an external force such as an electrical or gravitational force. In the case of spherical particles, the Stokes Einstein expression together with the Cunningham slip correction (Friedlander, 2000; Hinds, 1999) allows one to predict the drift velocity from knowing the particle diameter. In the case of nonspherical particles, the scalar friction coefficient for a sphere is replaced with the symmetric friction tensor leading to a dependence of the mobility

\* Corresponding author.

E-mail address: [georgewm@umd.edu](mailto:georgewm@umd.edu) (G.W. Mulholland).

on the particle orientation (Happel and Brenner 1983). Theoretical predictions of the particle mobility for nonspherical randomly oriented particles have been based on either the assumption of slow rotation relative to the aerosol relaxation time (Happel and Brenner 1983) or fast rotation (Li, Mulholland & Zachariah, 2014a). In this paper a model equation is proposed for studying the effect of the rotation rate on the particle drift velocity. One advantage of this approach is that the heuristic treatment of the essential physics using a one dimensional model avoids the complexity of the three dimensional coupled translational and rotational equations of motion.

It will be shown that in the case of free molecular dynamics, the drift velocity is affected by the rotation rate. However, for the case of continuum motion, the particle rotation is always in the slow rotation limit so that the expression given by Happel and Brenner is valid.

This paper focusses on the effect of rotation on the drift velocity of a nonspherical particle in air. There are two methods for computing the drift velocity. The most commonly used method is based on the steady state equation of motion for a nonspherical particle (Happel and Brenner, 1983). At steady state, the external force  $\vec{F}$  acting on the particle and the friction tensor  $\vec{K}$  are related by the following equation:

$$\vec{K}\vec{v} = \vec{F} \quad (1)$$

Thus, the drift velocity is given by:

$$\vec{v} = \vec{K}^{-1}\vec{F} \quad (2)$$

The expression for the orientation averaged drift velocity about the center of mass for non-skew particles is given by:

$$\langle \vec{v} \rangle = \frac{1}{3}(1/K_1 + 1/K_2 + 1/K_3)F\hat{k} = \frac{1}{K_h}F\hat{k}, \quad (3)$$

where the external force is in the direction of the unit vector  $\hat{k}$ . The quantity  $K_i$  is the  $i$ th principal component of the friction tensor and  $K_h$  is a shorthand expression for the harmonic mean given in expression after the 1st equality. This expression was derived by Happel and Brenner (1983) for the case of a gravitational external field. The nonskew property means that there is no coupling between the translational and rotational motion and that the particle possesses a center of hydrodynamic stress. Examples of nonskew particles include bodies of revolution such as cylinders and prolate and oblate ellipsoids.

Equation (3) has been widely used in computing the orientation averaged drift velocity for aerosols. Near the beginning of his review regarding the drag forces on nonspherical particles, Cheng (1991) presents the analog to Eq. (3) for the dynamic shape factor. Dahneke (1973a, 1973b, 1973c) used this expression for nonspherical particles in the continuum, free molecular, and transition regime. Larriba et al. (2013a) have used Eq. (3) for computing the orientationally averaged collision cross section for nanoparticles and complex ions along with the electrical mobility. Eq. (3) was used in the study of polystyrene doublets with monomer sizes ranging from 100 nm to 500 nm by Cheng, Allen, Gallegos, Yeh, and Peterson (1988) using Millikan cell measurements and by Kousaka, Endo, Ichitsubo, and Alonso (1996) and Zelenyuk, Cai and Imre (2006) based on electrical mobility measurements. Li, Mulholland and Zachariah (2012b, 2013) have used Eq. (3) in computing the mobility of randomly oriented carbon nanotubes and of gold nanorods. Eq. (3) has been applied to chains of spheres by Dahneke (1982) for a wide range of Knutson numbers and to agglomerates by Mackowski (2006) for the drag force computed in the free molecular limit by Monte Carlo simulation.

Li et al. (2014a) pointed out that Eq. (1) is not valid if the particle is rotating rapidly compared to the aerosol relaxation time. In this case the drift velocity is nearly independent of the orientation because there is not time for the drift velocity to adjust to the orientation dependent friction coefficient. Li et al. (2014a) derived the following expression for the drift velocity in the limit that the rotation time is much smaller than the aerosol relaxation time:

$$\langle \vec{v} \rangle = \frac{1}{1/3(K_1 + K_2 + K_3)}F\hat{k} = \frac{F\hat{k}}{K_{av}} \quad (4)$$

While this equation has not been previously used, there is an equivalent expression used in calculating the drift velocity of molecular ions based on computing the collision integral by using Chapman-Enskog theory (Ruotolo, Benesch, Sandercock, Hyung & Robinson, 2008, Shvartsburg and Jarrold 1996; Shvartsburg, Mashkevich, Baker & Smith, 2007; von Helden, Hsu, Gotts & Bowers, 1993). The drift velocity is related to the orientationally averaged collision integral. Li et al. (2014a) show that for nanorods in the free molecular limit, the expression for  $\langle \vec{v} \rangle$  in Eq. (4) is equivalent to the expression computed using the orientation averaged collision integral based on hard sphere collisions for randomly oriented ions.

There are also a number of studies (both theoretical and experimental) wherein the free molecular drag is assumed directly proportional to the orientationally averaged project area (PA) of a particle. The proportionality to the projected area is equivalent to Eq. (4) for the case of particles with a convex shape. Rogak, Flagan and Nguyen (1993) were the first to show experimentally for small agglomerates that the mobility diameter was approximately linearly related to PA. Exact linearity for the relationship between the drag and PA has not been shown for concave surfaces from which there can be multiple collisions of one gas molecule with the surface of a single particle. However, Zhang, Thajudeen, Larriba, Schwartzentruber, and Hogan (2012) show over a large range of cluster sizes in the free molecular limit that the ratio of the cross section to the

projected area for fractals is constant with a standard deviation on the order of 3% for all the simulations. This study included results for four fractal dimensions and for both diffuse and specular reflection.

In the same paper, Zhang et al. used dimensional analysis to arrive at a scaling equation for the scalar friction coefficient in the transition regime where the projected area is a key quantity in the definition of a Knudsen number for nonspherical particles. Direct Simulation Monte Carlo modelling was carried out to validate the scaling equation. The experimental studies by Gopalakrishnan, McMurry, and Hogan (2015) validated the scaling equation for low to high aspect ratio particles including gold nanorods, PSL doublets, and carbon nanotubes and by Thajudeen, Jeon and Hogan (2015) for TiO<sub>2</sub> aggregates over the mobility diameter range of 45 nm to 80 nm.

In the Discussion Section we will comment on the collision cross section measurements by Larriba et al. (2013b and 2015) for multiply charged polyethylene glycol chains and multiply charged ions of ionic liquids in regard to our model calculations on the effect of rotation on the drift velocity, or equivalently, on the collision cross section.

## 2. Model equation

(Equations (3) and 4) correspond to the two extremes of fast and slow rotation relative to the translational aerosol relaxation time. There is the unanswered question about the drift velocity for intermediate rotation rates. To provide a physical validation of the limiting expressions and to also treat the intermediate case, we pose the following 1-D model equation for a nonspherical particle both translating and rotating. It includes an inertial term, an orientation dependent friction coefficient to simulate the changes as the particle rotates, and an external force  $F$ :

$$m \frac{dv}{dt} = -(a + b \cos(\omega t))v + F = -K_m(\theta)v + F \quad (5)$$

The  $\cos(\omega t)$  term accounts for the orientation dependence of the model friction coefficient  $K_m$  where  $\theta = \omega t$ . One can think of  $\theta$  as the angle between the direction of the force and the major axis of particle. The constant  $a$  must be larger than  $b$  so that the friction coefficient does not vanish or become negative. This equation has the property that the drift velocity, averaged over one cycle for slow and fast rotation, correspond to the angle average of the inverse of the friction coefficient and to the average of the friction coefficient, respectively, in analogy to Eqs. (3) and (4). The slow rotation corresponds to the inertial term being zero and the fast rotation to the period for one cycle being much smaller than the minimum aerosol relaxation time  $\tau = m/K_m(\theta_{\max})$ .

$$\langle v \rangle_{\text{slow}} = \left[ \int \frac{d\theta}{K_m(\theta)} / \int d\theta \right] F = \frac{F}{K_{m,h}} \quad (6)$$

$$\langle v \rangle_{\text{fast}} = \left[ \int K_m(\theta) d\theta / \int d\theta \right]^{-1} F = \frac{F}{K_{m,av}} \quad (7)$$

Eqs. (6) and (7) are the scalar analogs of Eqs. (3) and (4). Carrying out the integrals from 0 to  $2\pi$ , one obtains the following limiting velocities:

$$\langle v \rangle_{\text{slow}} = \frac{1}{\sqrt{a^2 - b^2}} F \quad (8)$$

$$\langle v \rangle_{\text{fast}} = \frac{F}{a} \quad (9)$$

To solve for the time dependent drift velocity, it is convenient to express the differential equation in reduced form.

$$dv_r/dt_r + (1 + r \cos(\alpha t_r))v_r = 1, \quad (10)$$

where  $v_r = v/v_0$  and  $t_r = t/\tau$  with

$$v_0 = F\tau/m \quad (11)$$

$$\tau = m/a \quad (12)$$

$$r = b/a \quad (13)$$

$$\alpha = \omega\tau \quad (14)$$

The quantity  $\tau$  is the aerosol relaxation time,  $r$  relates to the magnitude of the harmonic term, and  $\alpha$  is a reduced rotation velocity.

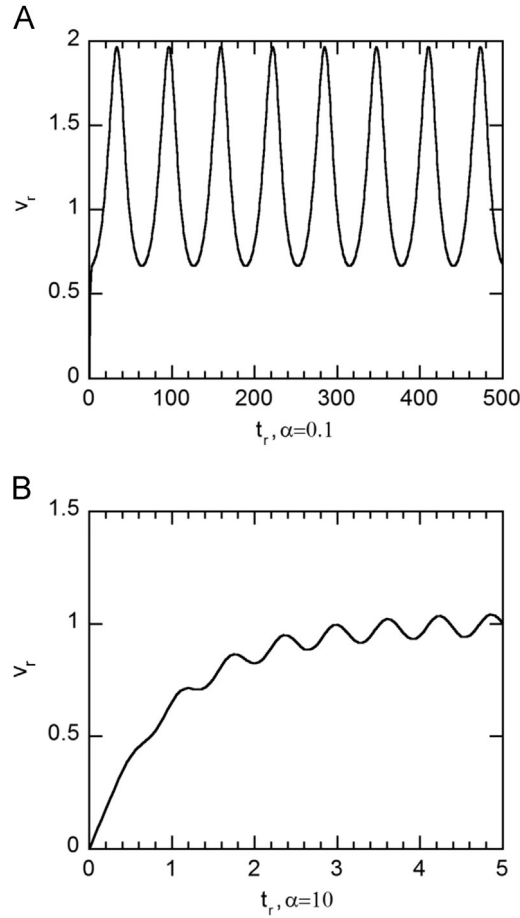


**Fig. 1.** Reduced drift velocity is plotted versus reduced time for low rotation velocity ( $\alpha=0.1$ , Plot A) and for high rotation velocity ( $\alpha=10$ , Plot B). In both cases the initial drift velocity is zero.

Solving the linear differential equation by determining an integrating factor and assuming the reduced drift velocity  $v_r$  is zero at  $t_r=0$ , one obtains:

$$v_r(t_r) = \int_0^{t_r} \exp\left(- (t_r - t'_r) - \frac{r}{\alpha} (\sin(\alpha t_r) - \sin(\alpha t'_r))\right) dt'_r \quad (15)$$

For the following calculation, it is assumed that  $r$  equals  $\frac{1}{2}$ . This results in the maximum to the minimum friction coefficient being 3. Our focus is on the behavior at low rotation velocity, where the theory of Brenner is correct, and the high rotation velocity,  $v_r$ , where the simply averaged expression is expected to be correct. In Fig. 1 we show the reduced drift velocity versus times for a value of the reduced rotation velocity ( $\alpha$ ) equal 0.1 and 10. The integration was carried out using Wolfram Mathematica<sup>1</sup> software. At the low rotation velocity, the drift velocity adjusts to the change in the friction coefficient so quickly that the acceleration term is only important at small times corresponding to a few percent of one oscillation. At high rotation velocity the drift velocity transient persists over three cycles. At longer times the drift velocity becomes periodic though the amplitude of the oscillations are small because the period of the oscillation is small compared to the particle relaxation time  $\tau$ . The period of the oscillation is equal to  $2\pi/\alpha$ .

The long time average reduced particle drift velocity,  $\langle v_r \rangle$ , is computed as:

$$\langle v_r \rangle = \int_T^{T+2\pi/\alpha} v_r(t) dt \quad (16)$$

where the integral is taken over a cycle starting at  $T$ , where  $T$  is large enough for  $v_r$  to have reached a constant cyclic pattern. This would be  $T \approx 3$  for  $\alpha=10$  and  $T \approx 400$  for  $\alpha = 0.1$  as indicated in Fig. 1. As shown in Fig. 2, the average drift velocity

<sup>1</sup> Certain trade names and company products are mentioned in the text in order to adequately specify the calculation method used. In no case does such identification imply recommendation or endorsement by the National Institute of Standards and Technology, nor does it imply that the software is the best available for the purpose.

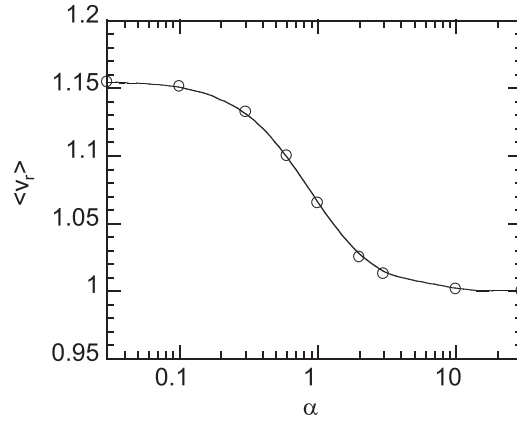


Fig. 2. Dependence of the reduced drift velocity on the rotation velocity for the coefficient of the harmonic term  $r=0.5$ .

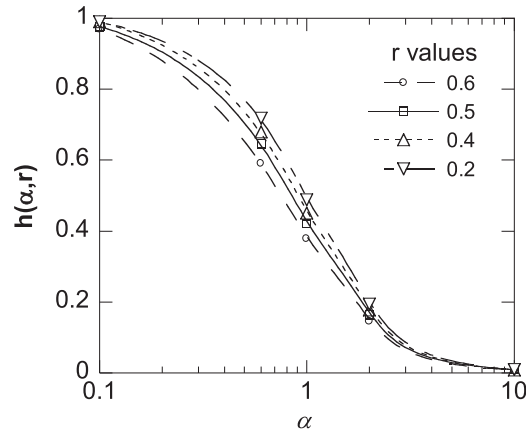


Fig. 3. Transition function  $h(\alpha, r)$  vs  $\alpha$  for a range of values of the harmonic term coefficient  $r$ .

approaches the limiting velocities predicted by Eqs. (8) and (9),  $2/\sqrt{3}$  ( $= 1.1547\cdots$ ) and 1, for low and high reduced rotational velocities (0.1 and 10) for  $r=1/2$ . The average drift velocity is not equal to the average of the peak and valley velocities because the  $v_r$  vs  $t_r$  curve is broader near the minimum than the peak (see Fig. 1 for  $\alpha=0.1$ ).

Above, we considered the quantity  $\langle v_r \rangle$  as a function of  $\alpha$ . It is also a function of the coefficient of the harmonic term,  $r$ . The dependence of  $\langle v_r \rangle$  on both  $r$  and  $\alpha$  can be given in term of a product of a function of  $r$ ,  $g(r)$ , and a transition function  $h(\alpha, r)$ , which is a monotonically decreasing function of  $\alpha$  with a value of 1 in the limit of small  $\alpha$  and a value of 0 in the limit of large  $\alpha$ :

$$\langle v_r \rangle = 1 + g(r)h(\alpha, r), \quad (17)$$

where

$$g(r) = \left(1 - (1 - r^2)^{1/2}\right) / (1 - r^2)^{1/2} \quad (18)$$

The function  $g(r)$  satisfies the small  $\alpha$  limit that  $\langle v_r \rangle = 1/(1 - r^2)^{1/2}$  (Eqs. (8) and (9)). It is seen from Fig. 3 that the function  $h(\alpha, r)$  has a weak dependence on  $r$ . This figure can be used together with Eqs. (17) and (18) to estimate the value of  $\langle v_r \rangle$  for a range of values of  $\alpha$  and  $r$ .

### 3. Rotation effect for nanorods

To relate the results of this model equation to the dynamics of an actual nonspherical particle, the relaxation time scales for the translational drift velocity and the rotational Brownian motion are needed. Here we consider as an example a circular cross section nanorod in the free molecular limit. The relaxation time for the translational motion (Hinds) for the case of a

non- spherical particle is estimated as:

$$\tau_t = m/K_h, \quad (19)$$

where  $K_h$  is computed using Eq. (3).

For Brownian rotation, we consider the case of rotation about the axis with the smallest rotation diffusion coefficient,  $D_{\min}$ . The variance of the angle of rotation  $\theta$  relative to an initial angle equal 0 is related to the diffusion coefficient and time  $t$  by the expression:

$$\langle \theta^2 \rangle = 2D_{\min}t \quad (20)$$

There is a degree of arbitrariness in the choice of the rotation relaxation time,  $\tau_r$ . Because of the symmetry for a rod, the full range of variation in the friction coefficient occurs over an angle range of 0 to  $\pi/2$ . We chose the rotation relaxation time as the time at which the standard deviation of the rotation angle is equal to 1 rad, which corresponds to be about half of the above angle range. This leads to the following estimate of the rotation relaxation time,  $\tau_r$ :

$$\tau_r = 1/(2D_{\min}) \quad (21)$$

The corresponding nanorod rotation velocity  $\omega_{nr}$  is estimated based on the square root of the angular variance as:

$$\omega_{nr} = \left[ \langle \theta^2 \rangle \right]^{1/2} / \tau_r = 2D_{\min}. \quad (22)$$

Finally, the reduced rotation velocity  $\alpha_{nr}$  is given by:

$$\alpha_{nr} = \omega_{nr} \tau_t = 2D_{\min} \tau_t \quad (23)$$

We compute  $\tau_t$  and  $D_{\min}$  for circular cross section nanorods with flat end caps and with diameter  $d_{nr}$  and length  $L_{nr}$  in the free molecular limit. The principle components of the friction tensor are, and  $K_1$  ( $= K_2$ ) for flow perpendicular to the major axis and  $K_3$ , for flow parallel to the major axis of the nanorod. These quantities are derived by Li et al. (2012a) based on Dahneke's scalar expression of drag force as a function of orientation angle (Dahneke, 1973b):

$$K_1 = \frac{\pi \eta d_{nr}^2}{2\lambda} \left[ \left( \frac{\pi-2}{4} \beta + \frac{1}{2} \right) f + 2\beta \right] \quad (24)$$

$$K_3 = \frac{\pi \eta d_{nr}^2}{2\lambda} \left[ \left( \beta + \frac{\pi}{4} - 1 \right) f + 2 \right], \quad (25)$$

where  $\eta$  is the gas viscosity,  $\lambda$  the mean free path of gas,  $f$  the momentum accommodation coefficient, and  $\beta$  the aspect ratio for the nanorod defined by  $L_{nr}/d_{nr}$ .

The rotational diffusion coefficient for a nanorod in the free molecular regime is (Li, Mulholland & Zachariah, 2014b):

$$D_{nr} = \frac{2k_B T \lambda}{\pi \eta L_{nr}^3 d_{nr} \left[ \left( \frac{1}{6} + \frac{1}{8\beta^3} \right) + f \left( \frac{\pi-2}{48} + \frac{1}{8\beta} + \frac{1}{8\beta^2} + \frac{\pi-4}{64\beta^3} \right) \right]} \quad (26)$$

where  $k_B$  is the Boltzmann constant and  $T$  is the absolute temperature.

The value of  $\tau_t$  is computed using Eqs. (3), (19), (24) and (25) and  $\omega_{nr}$  is computed from Eqs. (22) and (26). The calculations are based on a temperature of 296.2 K, pressure of 101.3 kPa, a viscosity of  $1.832 \times 10^{-5} \text{ kg m}^{-1} \text{ s}^{-1}$ , mean free path of  $6.730 \times 10^{-8} \text{ m}$ , density of  $1.000 \text{ kg m}^{-3}$ , and  $f$  of 0.9. As shown in Fig. 4, the value of  $\alpha_{nr}$  is greater than 1 for nanorods up to 16 nm diameter for  $\beta$  less than or equal to 3. Over this range of  $\alpha_{nr}$  the reduced rotation velocity is significantly affected by the rotation. For nanorods with diameters of at most 3 nm,  $\alpha_{nr}$  is greater than 1 for  $\beta$  up to 17. From Eqs. (19), (23) and (26) one finds that  $\alpha_{nr}$  is approximately proportional to  $\beta^{-3} d_{nr}^{-3}$ .

In our model calculation of particle drift velocity, we assumed  $r=0.5$ . It is of interest to compute the particle drift velocity based on the parameters for nanorods. From Eqs. (3) and (4) and noting that  $K_1=K_2$  for nanorods, we obtain the following expression for the ratio of the cycle average velocities,  $V_{ratio,nr}$ , in the limit of slow and fast rotation for nanorods:

$$V_{ratio,nr}(\beta) = \frac{\langle v_{nr} \rangle_{slow}}{\langle v_{nr} \rangle_{fast}} = \frac{1}{9} \left( 5 + 2 \left( \frac{K_1}{K_3} + \frac{K_3}{K_1} \right) \right) \quad (27)$$

From Eqs. (8) and (9), the ratio of the velocities is given by:

$$\frac{\langle v \rangle_{slow,model}}{\langle v \rangle_{fast,model}} = \frac{1}{\sqrt{1-r^2}} \quad (28)$$

For a fixed value of  $f$ , the asymptotic drift velocity ratio given by Eq. (27) is a function of only the aspect ratio  $\beta$ . The corresponding value of  $r$  is obtained by equating the nanorod expression for the velocity ratio with the model ratio. It is seen in Fig. 5 that the drift velocity ratio increases from a value of 1.0 to 1.133 as  $\beta$  increases from 1 to 10 and has a large  $\beta$  limit of 1.204 for a fixed momentum accommodation coefficient  $f=0.9$ . This value corresponds to a value of  $r$  equal 0.55 for the model equation as indicated in Fig. 5.

It is of interest to estimate the error resulting from using the low rotation velocity limit expression for the drift velocity, which is the most widely used expression, rather than the expression appropriate for the rotation velocity and translation relaxation time for the nanorods.

We express the percent error,  $\Delta(\alpha, r)$  as:

$$\Delta(\alpha, r) = 100(\langle v_r(\alpha, r) \rangle - \langle v_r(0, r) \rangle) / \langle v_r(0, r) \rangle \quad (29)$$

The results are shown in Table 1 where the two model parameters are expressed in terms of the nanorods diameter and aspect ratio. We computed  $v_r(\alpha, r)$  using Eq. (16).

In the Introduction it was stated that the slow rotation limit was valid for the continuum limit. To verify this, the values of the dimensionless rotation velocity  $\alpha_{cr}$  were computed for circular cross section rods in the continuum limit based on the

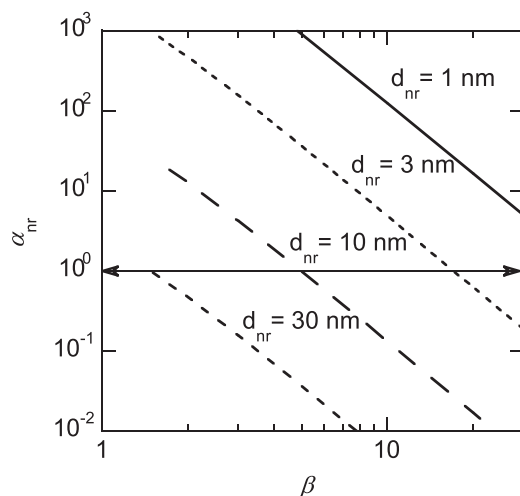


Fig. 4. The effect of cylinder diameter and aspect ratio on the reduced rotation velocity. The horizontal double arrow line is the demarcation between fast (above the line) and slow rotation region.

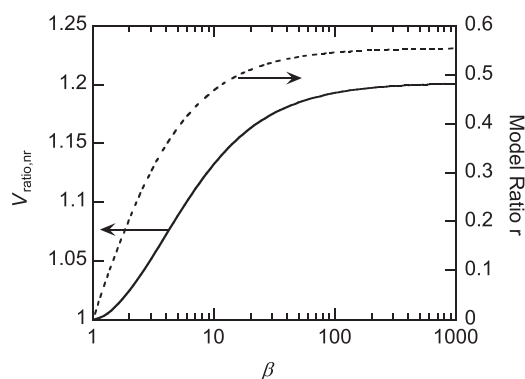


Fig. 5. The dependence of the ratio of the cycle average drift velocity for slow and fast rotation of a nanorod on its aspect ratio. Also the value of  $r$  for the model equation is given. The momentum accommodation coefficient  $f = 0.9$  is used.

Table 1

Percent error,  $\Delta$  (Eq. 29), from Neglecting Rotation for Nanorods.

$d_{nr}$	values of $\beta$					
	1.5	3	5	10	20	30
1	-0.84	-4.79	-8.13	-11.76	-14.06	-14.48
3	-0.84	-4.79	-8.13	-11.38	-5.31	-1.20
5	-0.84	-4.79	-8.01	-6.56	-0.68	0.00
10	-0.84	-4.26	-4.15	-0.53	0.00	0.00
20	-0.75	-1.06	-0.13	0.00	0.00	0.00
30	-0.23	-0.13	0.00	0.00	0.00	0.00

expressions for the diffusion coefficient given by [Ortega and de la Torre \(2003\)](#) and for the friction tensor given by [Batchelor \(1970\)](#). It was found that the values of  $\alpha_{cr}$  varied from a minimum of  $2.2 \times 10^{-4}$  to  $3.7 \times 10^{-7}$  for rod lengths over the range of 1  $\mu\text{m}$  to 100  $\mu\text{m}$  and  $\beta$  over the range of 2 to 10. So it is seen that the low rotation velocity limit value for the drift velocity is valid in the continuum limit.

#### 4. Discussion

For nanorods with diameters greater than 20 nm, the predicted error in using the low rotation limit for computing the drift velocity is at most 1% for any value of  $\beta$ . For smaller diameter nanorods, the error can be larger. The largest error is –14% for  $\beta$  equal 30 for a 1 nm diameter nanorod. For  $\beta$  equal 10, the errors are –11% and –7% for a 3 and 5 nm diameter nanorods.

The analysis of this paper relates to the drift velocity. The drift velocity is inversely proportional to the collision cross section. As the rotation velocity increases, the drift velocity decreases and the collision cross section increases. [Table 1](#) could be expressed in terms of percent changes in the collision cross section relative to the fast rotation limit by using the relation between the ratio of the slow to fast velocity limits and  $\beta$  ([Eq. \(27\)](#) and [Fig. 5](#)) together with the values in [Table 1](#).

As suggested by the plot of  $h(\alpha, r)$  in [Fig. 3](#), the fast rotation limit is approached within 1% for  $\alpha > 10$  and the slow rotation limit for  $\alpha < 0.05$ . This corresponds to a ratio of 200 for the  $\alpha$ 's in the two limits. [Li \(2012b\)](#) obtain a wider limit of 482 based on two times: The first, the time at which 50% of the particles have rotated by at least  $\pi/2$ , and the second, the time at which 10% of the particles have rotated by  $\pi/18$ . Both of these approaches are approximate, and as discussed below, a quantitative result would require the solution of the Langevin equations for the rotational and translational motion.

[Larriba and Hogan \(2013b\)](#) measured the mobilities of multiply charged polyethylene glycol chains. They found for a high aspect ratio structure with a nominal diameter of 1 nm and 70 monomer units that the measured mobility exceeded the predicted value by 10% for a diffuse hard sphere scattering model and by 4% for a model that also included a polarization potential. Their model uses the Happel – Brenner approach for computing the drag tensor (their [Eq. \(12\)](#)). This approach assumes a slow rotation velocity relative to the particle relaxation time. Modeling the structure as a nanorod with a 1 nm diameter and 10 nm length, we find that the nanorod is in the fast rotation limit (see [Table 1](#)) with the mobility decreased by about 12% from the slow rotation limit. So the rotation affect may be a partial cause of the difference between theory and experiment for the mobility of the multiply charged polyethylene glycol chains.

The study by [Li and Wang \(2003\)](#) indicates that the momentum accommodation coefficient  $f$  decreases for silver nanoparticles as the particle size decreases below 3 nm. This means that there is an increased fraction of specular collisions. [Larriba-Andaluz, Fernandez-Garcia, Ewing, Hogan, and Clemmer \(2015\)](#) measured the collision cross section of positively charged ions of ionic liquids 1-ethyl-3-methylimidazolium dicyanamide (EMIM-N(CN)<sub>2</sub>) and 1-ethyl-3-methylimidazolium tetrafluoroborate (EMIM-BF<sub>4</sub>) in N<sub>2</sub> using a differential mobility analyzer-mass spectrometer (DMA-MS) and in He using a drift tube mobility spectrometer-mass spectrometer (DT-MS). They found that the ratio of the collision cross section to the projected area,  $\Omega/PA$ , was about 1.40 independent of particle size for mass diameters over the range of 1 nm to 9 nm for nitrogen gas, while for helium gas, the ratio varied from about 1.07 for 1 nm diameter to about 1.25 for 9 nm. These ratios correspond to values for the momentum accommodation coefficient of 1.02, 0.18, and 0.64 obtained using the following relationship between  $\Omega/PA$  and  $f$ :

$$f = 8(\Omega/PA - 1)/\pi \quad (30)$$

For nanorods with a diameter of 1 nm and an aspect ratio of 10, the velocity ratios for these values of  $f$  are 1.10, 1.82, and 1.24. This demonstrates that in helium gas the error from using the slow rotation approximation is predicted to be much larger for small diameter nanorods than in nitrogen gas. The reason for the large change is from the large reduction in the friction coefficient for the nanorod aligned in the direction of the flow. The measurement of the electrical mobility of multiply charged polyethylene glycol chains in both helium and nitrogen would provide a test of the model predictions.

There is a caveat to the analysis in the preceding paragraph. [Eq. \(30\)](#) is based on Epstein's analysis that divides collisions into specular collisions and diffuse collisions. [Larriba-Andaluz et al. \(2015\)](#) show this is not an accurate description of realistic gas particle collisions. In fact, the inferred value of  $f$  from the cross section values is larger than 1.0, implying the unphysical result of more than 100% specular reflection. Still, we think that the qualitative trend predicted by this analysis regarding the velocity ratio is a useful first order treatment. Ultimately a theory is needed that incorporates both a realistic model of the gas particle interaction and particle rotation.

The dimensionless rotation velocity  $\alpha_{nr}$  is also affected by the choice of the background gas because it is proportional to  $(\lambda/\eta)^2$ . This would result in a seven fold increase in the  $\alpha_{nr}$  for helium compared to nitrogen assuming a momentum accommodation coefficient equal to 0.9. If the accommodation were smaller than 0.9, the value  $\alpha_{nr}$  would increase further; for example, for  $f$  equal 0.18, the predicted value of  $\alpha_{nr}$  increases by a factor 15 for a 1 nm diameter nanorod with  $\beta$  equal 10.

The aerosol relaxation time is proportional to the particle density. In the analysis above, it has been assumed the density is 1000 kg/m<sup>3</sup>. The relaxation time would increase in proportion to the density. For a silver nanorod with a density of 8000 kg/m<sup>3</sup>, the % deviation from the slow rotation limit would increase from –0.6% to –7% for a 10 nm diameter nanorod with an aspect ratio of 10 and from –0.2% to –5% for a 20 nm diameter nanoparticle with an aspect ratio of 5.

The analysis leading to the expressions for the diagonal components of the friction tensor in Eqs. (25) and (26) is based on the assumption that the nanorod is stationary during the collisions. Shvartsburg, Mashkevich & Siu (2000) included the effect of thermal rotation on the ion mobility. The following approximate expression for the change in the projected cross section of a square nanorod from the rotation of the nanorod is derived in Appendix B:

$$\frac{\Delta A_p}{A_p} = C \left[ \frac{m_g}{m_{nr}} \right]^{1/2} \quad (31)$$

The constant  $C$  was chosen to be 0.24 based on molecular dynamics simulations carried out by Shvatsburg et al. For a square cross section nanorod (1 nm  $\times$  1 nm) with a length of 10 nm, the predicted increase in the collision cross section for He, N<sub>2</sub>, A, Xe are 0.3%, 1.2%, 1.4%, and 2.5%. While this analysis is only valid to within about a factor of 2, it does suggest that at least for nitrogen gas, the thermal rotation does not affect the collision cross section or mobility by more than a couple percent for nanorods with an aspect ratio of 10 or greater and with diameters greater than 1 nm. For smaller nanorod type structures or for large atomic mas gases such as Xe, the effect may warrant a quantitative treatment to help understand the deviations observed between theory and experiment regarding the collision cross section for ionic liquids (Larriba-Andaluz, 2015) and for coulombically stretched polyethylene glycol chains (Larriba and Hogan, 2013a, 2013b).

There is a close relationship between the particle drift velocity and the particle diffusion coefficient. It is given by  $D = kT/f$  (Einstein 1905, Friedlander 2000), where  $f$  is the friction coefficient. In the case of nonspherical particles, a widely used expression for the translational diffusion coefficient is given by Landau and Lifshitz (1959):

$$D = kT [1/3(1/K_1 + 1/K_2 + 1/K_3)] = kT/K_h \quad (32)$$

This corresponds to the low rotation velocity limit. As the rotation velocity increases, the diffusion coefficient will decrease from the slow rotation limit value by the same percentage factor as the drift velocity decreases in this limit.

The above analysis is based on a model equation containing the essential physics of two time scales – one for translation and one for rotation. The choice of a  $\cos(\omega t)$  time dependence is not unique. Another viable choice is a  $\cos^2(\omega t)$  dependence based on the angular dependence for the equation of motion for a nanorod as discussed in Appendix A. Using the relationship between  $\cos^2(\omega t)$  and  $\cos(2\omega t)$ , this case reduces to the earlier treatment except the frequency is doubled. This results in a doubling of the values of  $\alpha$  used in computing  $h(\alpha, r)$  in Fig. 3 and an increase in the % error for larger values of the diameter and aspect ratio of the nanorod. For example, the errors increased from  $-5.3\%$  to  $-8.9\%$  for  $d_{nr} = 3$  nm and  $\beta = 20$  and from  $-4.2\%$  to  $-6.4\%$  for  $d_{nr} = 10$  nm and  $\beta = 5$ . The complete table of the modified values given in Appendix A show that for most cases the change is small. It is along the diagonal of the table that the changes are significant.

The two periodic functions considered give similar results suggesting that they can be useful in estimating the magnitude of a rotational effect on the drift velocity. If one were to choose another periodic function such as a square wave, the velocity ratio in the two limits will be unchanged and the midpoint value of the two velocities is expected to be near a value of 1 for the reduced rotation velocity. We expect a change in the steepness of the sigmoidal curve for  $h(\alpha, r)$  shown in Fig. 3 for a square wave. Still, this is a heuristic treatment of the effect of rotation. A quantitative treatment would be to use the Langevin equations for both translation and rotation to compute the drift velocity of a nanotube. In this case, the Brownian rotation would be accurately described.

## Acknowledgement

Dr. Trevor Saccucci assisted with the numerical integration of the model equation.

## Appendix A. Analysis of model equation for a $\cos^2\omega t$ periodic function

As is shown below, a  $\cos 2\theta$  dependence is obtained for the friction coefficient of a nanorod or other bodies of revolution. The  $z$  component of the equation of motion for an electric field in the  $z$  direction is given by:

$$m \frac{dv_z}{dt} = -\hat{k} \cdot (\vec{K}_s \cdot \hat{k} v_z) + qE \quad (A1)$$

where  $\hat{k}$  is the unit vector in the space-fixed  $z$  direction and  $\vec{K}_s$  is the friction tensor expressed in terms of the space fixed axes. For an arbitrary orientation of the body of revolution, there is the following relationship between the friction tensor expressed in terms of the principal components of the body fixed axes,  $\vec{K}_b$ , and the friction tensor in terms of the space fixed axes:

$$\vec{K}_s = \vec{R} \vec{K}_b \vec{R}^{-1} \quad (A2)$$

$$\vec{K}_b = \begin{pmatrix} K_1 & & \\ & K_1 & \\ & & K_3 \end{pmatrix} \quad (A3)$$

**Table A1**  
Percent Error,  $\Delta$  ( Eq. 29), from Neglecting Rotation for Nanorods for  $\alpha_1=2\alpha$ .

$d_{nr}$	values of $\beta$					
	1.5	3	5	10	20	30
1	−0.84	−4.79	−8.13	−11.76	−14.06	−14.74
3	−0.84	−4.79	−8.13	−11.62	−8.94	−3.21
5	−0.84	−4.79	−8.13	−9.75	−2.01	0.00
10	−0.84	−4.72	−6.37	−1.39	0.00	0.00
20	−0.81	−2.39	−0.76	0.00	0.00	0.00
30	−0.58	−0.57	0.00	0.00	0.00	0.00

$$\vec{R} = \begin{pmatrix} \cos \psi \cos \varphi - \cos \theta \sin \varphi \sin \psi & \cos \psi \sin \varphi - \cos \theta \cos \varphi \sin \psi & \sin \psi \sin \theta \\ -\sin \psi \cos \varphi - \cos \theta \sin \varphi \cos \psi & -\sin \psi \sin \varphi + \cos \theta \cos \varphi \cos \psi & \cos \psi \sin \theta \\ \sin \theta \sin \varphi & -\sin \theta \cos \varphi & \cos \theta \end{pmatrix} \quad (A4)$$

where  $\vec{R}$  is the unitary rotation matrix expressed in terms of the Euler angles,  $K_3$  is the principal value for flow parallel to the major axes, and the other two components ( $K_1=K_2$ ) for flow perpendicular to the principal axis. Carrying out the matrix multiplication in Eq. (A2) and substituting into Eq. (A1), one obtains:

$$m \frac{dv_z}{dt} = -[K_1 - (K_1 - K_3) \cos^2 \theta] v_z + qE \quad (A5)$$

Using the relation between  $\cos^2 \theta$  and  $\cos(2\theta)$ , we obtain an expression similar to Eq. (5), our model equation.

$$m \frac{dv_z}{dt} = -[1/2(K_1 + K_3) + 1/2(K_1 - K_3) \cos 2\theta] v_z + qE = -[a_1 + b_1 \cos 2\theta] v_z + qE \quad (A6)$$

Substituting  $\omega t$  for  $\theta$  we obtain an equation identical in form to Eq. (5) except with twice the frequency. This change in frequency results in a doubling in the dimensionless rotation velocity.

$$\alpha_1 = 2\omega\tau \quad (A7)$$

We have computed the modified results for the reduced drift velocity using Eqs. (17) and (18). The value of  $h(\alpha_1, r)$  is determined from Fig. 3 using  $\alpha_1 = 2\alpha$ . The results for the percent error from using the low velocity limit are presented in Table A1.

We point out a subtlety in the above analysis. The expression for the velocity ratio given by Eq. (27) is the correct expression for a nanorod and is based on Eqs. (3) and (4), which include the tensor expression for the friction coefficient and the averaging over the Euler angles. Eq. (28) is an approximate expression based on a scalar average given by Eqs. (6) and (7). To illustrate the difference in the two expressions, we compute the velocity ratio for the nanorod for the case  $\beta = 10$ . From Eq. (27), we obtain  $V_{ratio}$  (Eq. (27)) = 1.133. The second approach is to compute  $r_1$  as the ratio  $b_1/a_1 = 0.361$  (from Eq. (A6)), and then use Eq. (28) to compute  $V_{ratio}$  (Eq. (27)) = 1.072. The increase from unity for the correct expression is almost twice the increase for the scalar analysis. A value of  $r$  equal 0.470 substituted into Eq. (28) will give the correct velocity average. Our approach is to compute the value of  $r$  that gives the correct velocity ratio and use this value in the average reduced velocity as a function of the reduced rotation velocity  $\alpha$ .

## Appendix B. Derivation of approximate equation for the effect of rotation velocity on the collision cross section

For simplicity we consider a square cross section nanorod ( $d \times d$ ). As the nanorod rotates perpendicular to the linear trajectory of a gas molecule, it is possible that the side surface of the nanorod will collide with the gas molecule. This would require the molecule to start near the nanorod surface and then collide with the rotating nanorod as it moves the distance equal to the thickness of the nanorod. A qualitative estimate of the increase in the cross section relative to no rotation based on the time  $\Delta t$  for the molecule to travel a distance  $d$  and the distance  $\Delta d$  rotated in this time.

$$\Delta t = d/v_z \quad (B1)$$

$$\Delta d = r\omega\Delta t, \quad (B2)$$

where  $v_z$  is the molecular velocity in the z-direction,  $\omega$  the rotation velocity of the nanorod, and  $r$  the distance from the center of the nanorod to an arbitrary point. We replace  $r$  with the average value  $R/2$ , where  $R$  is the distance from the center of the nanorod to its end, and estimate  $v_z$  and  $\omega$  using the equipartition of energy where  $I$  is the moment of inertial and  $m_r$  the mass of the rod assuming a density of 2000 kg/m<sup>3</sup>.

$$v_z = \sqrt{kT/m_g} \quad (B3)$$

**Table B1**

Fractional change in the nanorod cross section as a function of the molecular mass.

Gas	Mass of gas kg/molecule	$\Delta d/d$
He	3.32E-27	0.003
Nitrogen	4.65E-26	0.012
Argon	6.64E-26	0.014
Xenon	2.18E-25	0.025

$$\omega = \sqrt{kT/I} = \sqrt{3kT/(m_r R^2)} \quad (\text{in the slender rod limit}) \quad (\text{B4})$$

Substituting from Eqs. (B1), (B3), and (B4) into Eq. (B2), we obtain:

$$\Delta d = Cd \left[ \frac{m_g}{m_r} \right]^{1/2} \quad (\text{B5})$$

The proportionality constant  $C$  is chosen to be 0.24 to give the correct increase in cross section for the rotation of a chain of 10 carbon atoms (Shvartsburg et al., 2000) in Xenon gas. In Table B1 below, we show the predicted percentage increase in the collision cross section for 4 different gases. Since the collision length of the nanorod is not affected by rotation, the percentage change in the cross section area,  $\Delta A_p/A_p$ , is equal to the percentage change in  $d$ .

We comment that this analysis is qualitatively consistent with the molecular dynamics results of Shvartsburg et al. for trends regarding the effects of the molecular weight of the gas and the mass of the nanorod on the fractional change in  $\Delta d/d$ . However, this analysis is not able to predict the nanorod length giving the peak effect for a fixed diameter.

## References

- Batchelor, G. K. (1970). Slender-body theory for particles of arbitrary cross-section in Stokes flow. *Journal of Fluid Mechanics*, 44, 419–440.
- Cheng, Y. S., Allen, M. D., Gallegos, D. P., Yeh, H. C., & Peterson, K. (1988). Drag force and slip correction of aggregate aerosols. *Aerosol Science and Technology*, 8(3), 199–214.
- Cheng, Y. S. (1991). Drag forces on nonspherical aerosol-particles. *Chemical Engineering Communications*, 108, 201–223.
- Dahneke, B. E. (1973a). Slip correction factors for nonspherical bodies—i introduction and continuum flow. *Journal of Aerosol Science*, 4, 139–145.
- Dahneke, B. E. (1973b). Slip correction factors for nonspherical bodies—ii free molecule flow. *Journal of Aerosol Science*, 4, 147–161.
- Dahneke, B. E. (1973c). Slip correction factors for nonspherical bodies—iii the form of the general law. *Journal of Aerosol Science*, 4, 163–170.
- Dahneke, B. E. (1982). Viscous resistance of straight-chain aggregates of uniform spheres. *Aerosol Science and Technology*, 8, 179–185.
- Einstein, A. (1905). Über die von der molekular-kinetischen theorie der wärme geforderte bewegung von in ruhenden flüssigkeiten suspendierten teilchen. *Annalen der Physik*, 17, 549.
- Friedlander, S. K. (2000). *Smoke, dust, and haze, fundamentals of aerosol dynamics* (2nd ed.). New York and Oxford: Oxford University Press 32.
- Gopalakrishnan, R., McMurry, P. H., & C.J. Hogan, C. J. (2015). The electrical mobilities and scalar friction factors of modest to high aspect ratio particles in the transition regime. *Journal of Aerosol Science*, 82, 24–39.
- Happel, J., & Brenner, H. (1983). *Low reynolds number hydrodynamics* (1st paperback ed.). The Hague: Martinus Nijhoff 205–207.
- Hinds, W. C. (1999). *Aerosol technology properties, behavior, and measurement of airborne particles* (2nd ed.). New York: John Wiley and sons, Inc 111.
- Kousaka, Y., Endo, Y., Ichitubo, H., & Alonso, M. (1996). Orientation-Specific dynamic shape factors for doublets and triplets of spheres in the transition regime. *Aerosol Science and Technology*, 24(1), 36–44.
- Landau, L. D., & Lifshitz, E. M. (1959). *Fluid mechanics* (p. 228) Reading, Mass: Addison- Wesley Publishing Co. Inc. 228
- Larriba, C., & Hogan, C. J., Jr. (2013a). Free molecular collision cross section calculation methods for nanoparticles and complex ions with energy accommodation. *Journal of Computational Physics*, 251, 344–363.
- Larriba, C., & Hogan, C. J. (2013b). Ion mobilities in diatomic gases: measurement vs. prediction with non-specular scattering models. *The Journal of Physical Chemistry A*, 117, 3887–3901.
- Larriba-Andaluz, C., Fernandez-Garcia, J., Ewing, M. A., Hogan, C. J., & Clemmer, D. E. (2015). Gas molecule scattering & ion mobility measurements for organic macro-ions in He versus N<sub>2</sub> environments. *Physical Chemistry Chemical Physics*, 17(22), 15019–15029.
- Li, M., Mulholland, G. W., & Zachariah, M. R. (2012a). The effect of orientation on the mobility and dynamic shape factor of charged axially symmetric particles in an electric field. *Aerosol Science and Technology*, 46, 1035–1044.
- Li, M. (2012b). *Quantifying particle properties from ion-mobility measurements (Dissertation)*. College Park: University of Maryland. <http://hdl.handle.net/1903/13627>.
- Li, M., You, R., Mulholland, G. W., & Zachariah, M. R. (2013). Mobility of gold rods in an electric field. *Aerosol Science and Technology*, 47, 1101–1107.
- Li, M., Mulholland, G. W., & Zachariah, M. R. (2014a). Understanding the mobility of a nonspherical particle. *Phys Rev E*, 89, 022112.
- Li, M., Mulholland, G. W., & Zachariah, M. R. (2014b). Rotational diffusion coefficient (or rotational mobility) of a nanorod in the free-molecular regime. *Aerosol Science and Technology*, 48, 139–141.
- Li, Z., & Wang, H. (2003). Drag force, diffusion coefficient, and electric mobility of small particles. II. Application. *Physical Review E*, 68, 612071.
- Mackowski, D. W. (2006). Monte Carlo simulation of hydrodynamic drag and thermophoresis of fractal aggregates of spheres in the free-molecule flow regime. *Journal of Aerosol Science*, 37, 242–259.
- Ortega, A., & de la Torre, J. G. (2003). Hydrodynamic properties of rodlike and disklike particles in dilute solution. *Journal of Chemical Physics*, 119(18), 9914–9919.
- Rogak, S. N., R.C. Flagan, R. C., & Nguyen, H. V. (1993). The Mobility and Structure of Aerosol Agglomerates. *Aerosol Science and Technology*, 18(1), 25–47 (1993).
- Ruotolo, B. T., Benesch, J. L. P., Sandercock, A. M., Hyung, S. J., & Robinson, C. V. (2008). Ion mobility-mass spectrometry analysis of large protein complexes. *Nature Protocols*, 3, 1139–1152.
- Shvartsburg, A. A., & Jarrold, M. F. (1996). An exact hard-spheres scattering model for the mobilities of polyatomic ions. *Chemical Physics Letters*, 261(1–2), 86–91.

- Shvartsburg, A. A., Mashkevich, S. V., Baker, E. S., & Smith, R. D. (2007). Optimization of algorithms for ion mobility calculations. *Journal of Physical Chemistry A*, *111*(10), 2002–2010.
- Shvartsburg, A. A., S.V. Mashkevich, S. V., & Siu, K. W. M. (2000). Incorporation of thermal rotation of drifting ions into mobility calculations: Drastic effect for heavier buffer gases. *Journal of Physical Chemistry A*, *104*(42), 9448–9453.
- Thajudeen, T., Jeon, S., & Hogan, C. J. (2015). The mobility of flame synthesized aggregates/agglomerates in the transition regime. *Journal of Aerosol Science*, *80*, 45–57.
- von Helden, G., Hsu, M. T., Gotts, N., & Bowers, M. T. (1993). Carbon cluster cations with up to 84 atoms: structures, formation mechanism, and reactivity. *J Phys Chem*, *97*(31), 8182–8192.
- Zelenyuk, A., Cai, Y., & Imre, D. (2006). From agglomerates of spheres to irregularly shaped particles: determination of dynamic shape factors from measurements of mobility and vacuum aerodynamic diameters. *Aerosol Science and Technology*, *40*, 197–217.
- Zhang, C., Thajudeen, T., Larriba, C., Schwartzentruber, T. E., & Hogan, C. J. (2012). Determination of the scalar friction factor for non-spherical particles and aggregates across the entire knudsen number range by direct simulation Monte Carlo (DSMC). *Aerosol Science and Technology*, *46*, 1065–1078.